



Received: 2016.01.29
Accepted: 2017.04.06
Published: 2017.12.15

Authors' Contribution:

- A** Study Design
- B** Data Collection
- C** Statistical Analysis
- D** Data Interpretation
- E** Manuscript Preparation
- F** Literature Search
- G** Funds Collection

Iterative Reconstruction as a Method for Optimisation of Computed Tomography Procedures

Maria Staniszewska^{1ACDF}, Dariusz Chrusciak^{2BCE}

¹ Department of Medical Imaging Techniques, Medical University, Łódź, Poland

² Department Radiation Protection, Holy-Cross Oncological Centre, Kielce, Poland

Author's address: Maria Staniszewska, Department of Medical Imaging Techniques, Medical University, Łódź, Poland,
e-mail: maria.staniszewska@umed.lodz.pl

Background:

Computed tomography (CT) is still commonly regarded as a method that causes a high radiation exposure. For that reason, producers intensively try to find new solutions for dose reduction while maintaining a high diagnostic value of images. One of the recent strategies focuses on CT image reconstruction. Iterative reconstruction (IR) is an alternative for filtered back projection (FBP) that is commonly used today.

The aim of the article is to demonstrate and compare the effects of two IR algorithms on dose value and image details.

Material/Methods:

Investigations were performed on two 128 multi-detector (MDCT) CT scanners: – iCT (Philips Healthcare with iDose⁴); – Definitions AS+ (Siemens Medical Solutions with SAFIRE system).

The measurements involved: – image quality indicators for the CATPHAN 600 phantom; – dosimetric indicators of exposure (DLP i CTDI_{vol}).

Results:

The signal-to-noise ratios (SNR) in the images reconstructed with IR and FBP were analysed, and the SNR(IR)/SNR(FBP) ratios were calculated and correlated with CTDI_{vol} values. The effects of IR and FBP algorithms on low-contrast resolution were also compared in relation to CTDI_{vol} values. The smallest diameter of supra-slice objects in the Catphan phantom were taken into consideration.

Conclusions:

Both iterative algorithms definitely improved the visibility of low-contrast objects in comparison to a standard algorithm (FBP) with similar exposure parameters.

These algorithms allow an 80% reduction of the CTDI_{vol} value while maintaining an acceptable visibility of low-contrast objects. However, the results obtained with each of the studied iterative algorithms differ.

MeSH Keywords:

Image Processing, Computer-Assisted • Radiation Dosage • Tomography, X-Ray Computed

PDF file:

<http://www.polradiol.com/abstract/index/idArt/903557>

Background

Computed tomography (CT) is still commonly regarded as a method that causes a high radiation exposure. For that reason, producers intensively try to find new solutions for dose reduction while maintaining a high diagnostic value of images.

Earlier approaches relied on optimization of CT exposure parameters (also special paediatric protocols) and automatic tube-current modulation [1,2].

A newer dose reduction strategy focuses on optimization of CT image reconstruction. To date, most of CT scanners have used filtered back projection (FBP) as the algorithm for image reconstruction. FBP assumes that the acquired projection data are free of noise. Consequently, after mathematical filtering of projection data (e.g. smoothing or

edge-enhancement), they are projected back into image space to reconstruct the imaged volume. The FBP algorithm is fast and produces acceptable images in most situations.

However, when radiation dose is lowered, FBP-reconstructed images are highly noisy [3]. Iterative reconstruction (IR) is an alternative image reconstruction method that allows imaging at lower doses while maintaining image quality comparable to routine-dose FBP.

The concept of IR is well known, and the first IR algorithms were elaborated already in the 1970s to good effect. Due to the limited computational power of early CT workstations, the image creation process was very slow and the subsequently elaborated algorithm was quicker; it was the filtered back projection (FBP) algorithm, which has been successfully applied to date, even for quick multi-row CT scanners. A relatively high level of image noise is a disadvantage of the FBP algorithm. This results from the necessity of raw image data interpolation and is the cause of higher radiation doses to which patients are exposed in order to achieve good quality diagnostic images.

The improved computational effectiveness of CT reconstruction workstations permitted the introduction of IR. Consequently, all major CT manufacturers have recently implemented new IR algorithms for CT imaging as the best solution for dose reduction that does not compromise image quality.

Full iterative reconstruction consists of forward and backward reconstruction and thus operates in the raw data domain and image data domain. Simpler algorithms iterate successively in the raw data domain and then in the image data domain. The result of IR in the raw data domain is transmitted to the image domain by back projection [3].

There are differences in the approach to IR algorithms of different vendors. Each vendor has its own uniquely named IR technique, and the main CT vendors compete to achieve the lowest possible radiation exposure [4].

This article presents the effects of two IR algorithms of the same level of computational complexity (installed on the same CT workstations) on the image quality - dose exposure relationship in comparison to FBP algorithms.

A special aim of the article is to demonstrate the benefit of iterative algorithms for optimization of exam results in comparison to the FBP algorithm when routinely used exposure parameters are chosen.

Materials and Methods

Investigations were performed with two CT scanners:

- iCT scanner (Philips Healthcare with iDose⁴);
- Definitions AS+ (Siemens Medical Solutions with SAFIRE system).

Both IR solutions operate successively in the raw data domain and then in the image domain.

Both IR systems are multilevel: iDose⁴ has 7 levels and SAFIRE has 5 levels, corresponding to the number of iterative loop repetitions.

The workstations of the both scanners can independently use the FBP algorithm.

A starting point for the investigations was to set the exposure parameters to those commonly chosen for CT examinations of the trunk in adult patients:

high voltage $U=120$ kV, anode current $I=500$ mA, rotation time $t_{\text{rot}}=0.5$ s, pitch $p\approx 1$.

Both scanners have 128 active detector rows of the unit width $\Delta z=0.625$ mm for iCT and $\Delta z=0.6$ mm for Definition AS+, respectively.

The measurements involved:

- image quality indicators for the CATPHAN 600 phantom,
- dosimetric indicators of exposure (DLP i CTDI_{vol}).

For the dosimetric measurements, the Barracuda device (RTI, Sweden) and the HEAD 5-holes phantom ($\phi=16$ cm) were applied.

The following indicators of image quality were evaluated:

- low-contrast resolution (in the CATPHAN phantom the so-called supra-slice and sub-slice objects),
- high-contrast resolution (i.e. space resolution),
- signal-to-noise ratio (SNR).

SNR was evaluated for a region-of-interest (ROI) of 100 mm² placed in the area surrounding the objects of a nominal contrast level (CL) of 1%. In this ROI, the Hounsfield numbers and their standard deviations were interpreted as the signal level and the level of noise, respectively.

Independently, computed tomography dose index (CTDI) was calculated as the dosimetric indicator of CT exposure. For multi-row CT scanners, CTDI is calculated according to the following formula

$$CTDI_{vol} = \frac{\overline{DLP_{wz}}}{N \cdot \Delta z \cdot p}$$

where

N - number of active rows,

Δz - width of the single detector,

p - pitch,

$\overline{DLP_{wz}}$ the mean weighted value of dose length product (\overline{DLP})

$$\overline{DLP_{wz}} = \frac{1}{3} \overline{DLP_c} + \frac{2}{3} \overline{DLP_p},$$

$\overline{DLP_c}$ dose length product in the central hole of the phantom,

$\overline{DLP_p}$ dose length product in the peripheral holes of the phantom.

CTDI_{vol} should be understood as the absorbed dose averaged for the whole scanned volume. Thus, this value estimates radiation risk in patients undergoing an exam with given exposure parameters.

Table 1A. iCT (Philips) Determinants of image quality and CT dose index for exposure parameters U=120 kV, I_{xtot}=249 mAs.

Algorithm of image reconstruction	SNR	Low-contrast resolution (*)		Spatial resolution (**) (the smallest detectable distance) [cm]	CTDI _{vol} [mGy]
		Supra-slice objects at 1% contrast level	Sub-slice objects 3 mm height		
FBP	7.7	3 mm	5 mm	0.063	36.0
IDose-2	9.0	3 mm	5 mm		
IDose-4	11.0	3 mm	5 mm		
IDose-6	13.8	2 mm	3 mm		

* Diameter (in mm) of the smallest differentiable object is given; ** value after reconstruction using mathematical „bone” filter.

Table 2A. iCT (Philips) Determinants of image quality and CT dose index for exposure parameters U=120 kV, I_{xtot}=149 mAs.

Algorithm of image reconstruction	SNR	Low-contrast resolution (*)		Spatial resolution (**) (the smallest detectable distance) [cm]	CTDI _{vol} [mGy]
		Supra-slice objects at 1% contrast level	Sub-slice objects 3 mm height		
FBP	8.3	4 mm	7 mm	0.063	21.5
IDose -2	9.8	3 mm	7 mm		
IDose -4	11.6	3 mm	7 mm		
IDose -6	14.7	3 mm	5 mm		

* Diameter (in mm) of the smallest differentiable object is given; ** value after reconstruction using mathematical „bone” filter.

Table 3A. iCT (Philips) Determinants of image quality and CT dose index for exposure parameters U=80 kV, I_{xtot}=149 mAs.

Algorithm of image reconstruction	SNR	Low-contrast resolution (*)		Spatial resolution (**) (the smallest detectable distance) [cm]	CTDI _{vol} [mGy]
		Supra-slice objects at 1% contrast level	Sub-slice objects 3 mm height		
FBP	2.2	9 mm	no	0.063	7.3
IDose-2	2.7	9 mm	no		
IDose-4	3.1	8 mm	no		
IDose-6	3.9	6 mm	no		

* Diameter (in mm) of the smallest differentiable object is given; ** value after reconstruction using mathematical „bone” filter.

The measurements were performed for the three following exposure settings:

120 kV and 250 mAs, 120 kV and 150 mAs and 80 kV and 150 mAs.

CATPHAN images were reconstructed using successively the following algorithms:

- for iCT: FBP, iDose⁴ – level 2, iDose⁴ – level 4 and iDose⁴ – level 6,
- for Definition AS+: FBP, SAFIRE – level 2, SAFIRE – level 3, SAFIRE – level 5.

CATPHAN images were recorded with an intentionally thin reconstructive layer of 3 mm, corresponding to the smallest low-contrast sub-slice objects (i.e. 3 mm height) chosen for the analysis.

Results

The results corresponding to the particular settings of exposure parameters are given:

- in Tables 1A, 2A, and 3A for iCT and
- in Tables 1B, 2B, and 3B for Definition AS+.

As the main aim of the study was to evaluate the effects of IR algorithms in relation to the FBP algorithm, the SNRs in the images reconstructed under both algorithms were analysed; SNR, as defined above, was used as a measure of image quality. Thus, for particular levels of the IR algorithms, the ratios SNR(IR)/SNR(FBP) were calculated and correlated with CTDI_{vol} values. The results are presented in Figures 1 and 2 for iCT and Definition AS+, respectively.

As an optimal X-ray imaging procedure should provide a clinically useful image at a reasonably low dose to the

Table 1B. Definition AS+ (Siemens) Determinants of image quality and CT dose index for exposure parameters U=120 kV, Ixt_{rot}=250 mAs.

Algorithm of image reconstruction	SNR	Low-contrast resolution (*)		Spatial resolution (**) (the smallest detectable distance) [cm]	CTDI _{vol} [mGy]
		Supra-slice objects at 1% contrast level	Sub-slice objects 3 mm height		
FBP	14.7	3 mm	7 mm	0.071	39.3
SAFIRE-2	13.8	3 mm	7 mm		
SAFIRE-3	17.8	3 mm	7 mm		
SAFIRE-4	18.8	3 mm	7 mm		

* Diameter (in mm) of the smallest differentiable object is given; ** value after reconstruction using mathematical „bone“ filter.

Table 2B. Definition AS+ (Siemens) Determinants of image quality and CT dose index for exposure parameters U=120 kV, Ixt_{rot}=150 mAs.

Algorithm of image reconstruction	SNR	Low-contrast resolution (*)		Spatial resolution (**) (the smallest detectable distance) [cm]	CTDI _{vol} [mGy]
		Supra-slice objects at 1% contrast level	Sub-slice objects 3 mm height		
FBP	10.4	4 mm	7 mm	0.071	23.7
SAFIRE-2	12.8	4 mm	7 mm		
SAFIRE-3	13.6	3 mm	7 mm		
SAFIRE-4	16.6	3 mm	7 mm		

* Diameter (in mm) of the smallest differentiable object is given; ** value after reconstruction using mathematical „bone“ filter.

Table 3B. Definition AS+ (Siemens) Determinants of image quality and CT dose index for exposure parameters U=80 kV, Ixt_{rot}=150 mAs.

Algorithm of image reconstruction	SNR	Low-contrast resolution (*)		Spatial resolution (**) (the smallest detectable distance) [cm]	CTDI _{vol} [mGy]
		Supra-slice objects at 1% contrast level	Sub-slice objects 3 mm height		
FBP	2.8	12 mm	no	0.071	6.8
SAFIRE-2	3.8	9 mm	no		
SAFIRE-3	4.0	6 mm	no		
SAFIRE-4	4.5	6 mm	no		

* Diameter (in mm) of the smallest differentiable object is given; ** value after reconstruction using mathematical „bone“ filter.

patient, such an evaluation was performed for the results obtain in our study.

The effects of the IR and FBP algorithms for a low-contrast resolution were compared in relation to CTDI_{vol} values. The smallest diameters of supra-slice objects in the Catphan phantom were taken into consideration. The appropriate data are given in Table 4. Correlation between reduction of CTDI_{vol} and relative difference in low contrast (LC) is presented in Figure 3.

Ømin(FBP), Ømin (IR):

– the smallest diameters of supra-slice objects in the Catphan phantom visible at the FBP algorithm and IR algorithms (at the highest analysed level), respectively;
iCT, Def.AS+ – types of the CT scanners.

Discussion

Iterative reconstruction algorithms are offered now by four major CT vendors. These are different software solutions that are copyright protected.

While a multitude of reports promise that IR algorithms to enhance diagnostic performance and reduce radiation exposure, examples of the latter are limited in daily clinical practice.

It should be underlined that these benefits are evaluated through the diagnostic value of clinical images. Attention is given to image quality and especially to noise reduction. The latter is estimated as 13% to 50% in neurological or cardiac CT exams [6–8].

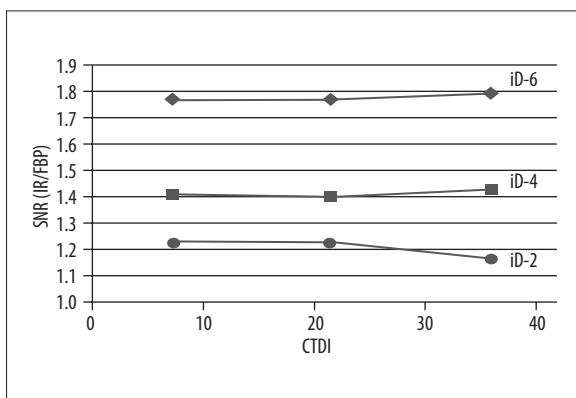


Figure 1. SNR(IR)/SNR(FBP) for iCT (Philips). ID-2 – IR algorithm at level 2 (Pearson’s coefficient for linear approximation $R^2=0.76$); ID-4 – IR algorithm at level 4 (Pearson’s coefficient for linear approximation $R^2=0.43$); ID-6 – IR algorithm at level 6 (Pearson’s coefficient for linear approximation $R^2=0.76$).

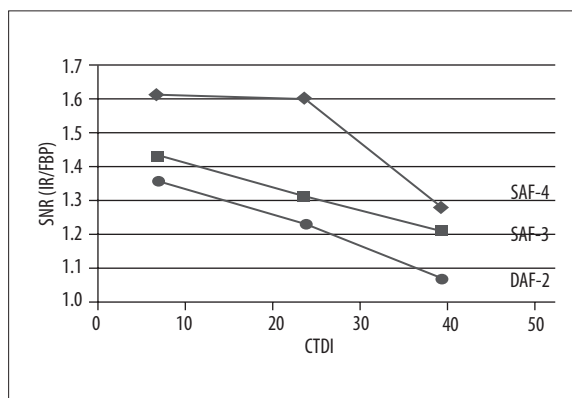


Figure 2. SNR(IR)/SNR(FBP) for Definition AS+ (Siemens). SAF-2 – IR algorithm at level 2 (Pearson’s coefficient for linear approximation $R^2=0.99$); SAF-3 – IR algorithm at level 3 (Pearson’s coefficient for linear approximation $R^2\approx 1$); SAF-4 – IR algorithm at level 4 (Pearson’s coefficient for linear approximation $R^2=0.75$).

Table 4. Visualization of the smallest supra-slice low-contrast objects at the FBP algorithm and the highest level of IR algorithm.

iCT			Definition AS+		
CTDI _{vol} [mGy]	\emptyset_{min} [mm]	Relative difference	CTDI _{vol} [mGy]	\emptyset_{min} [mm]	Relative difference
36.0	FBP --> 3 IDose-6 --> 2	30%	39.3	FBP --> 3 SAFIRE-4 --> 3	0%
21.5	FBP --> 4 IDose-6 --> 3	25%	23.7	FBP --> 4 SAFIRE-4 --> 3	25%
7.3	FBP --> 9 IDose-6 --> 6	30%	6.8	FBP --> 12 SAFIRE-4 --> 6	50%

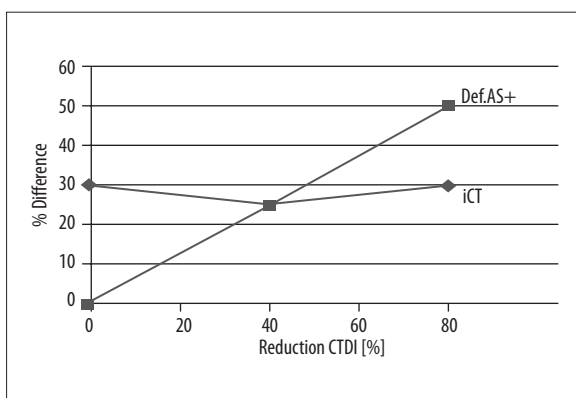


Figure 3. Correlation between reduction of CTDI_{vol} and relative difference in low contrast (LC): % difference = $\emptyset_{min}(FBP) - \emptyset_{min}(IR) / \emptyset_{min}(FBP)$ [%]. Reduction of CTDI = $(MaxCTDI - CTDI(i)) / MaxCTDI$ [%].

It should be also noted that spatial resolution of CT images is high and should not change due to the application of reconstructive algorithms. Thus, increased spatial resolution does not prove that IR algorithms perform better than FBP [8,9].

In the study by Yu et al. [10], image quality of abdominal CT with iDose⁴ and FBP was compared subjectively and objectively, and about a 20% reduction of image noise was found. This comparison did not include a dose evaluation.

Dose reduction can also be evaluated on the basis of clinical scans, and then it ranges between 7% and 80% depending on the CT scanner used [9,11–13].

Moreover, in principle, clinical image evaluation is dependent on diagnostic requirements and is not absolutely objective.

Consequently, a fully objective evaluation of the effects of IR algorithms should be performed using standard test objects for both image control and dose level.

Such standard objects are the Catphan phantom for image control and CT dosimetric phantoms. Standard phantoms were used for measurements of CTDI_{vol} and analysis of quality of image in this study. Thus, anatomical variation seen in patients and subjective image evaluation do not confound our results.

Moreover, our investigations concern the effects of two IR algorithms that are mathematically similar and which are used on technically comparable CT scanners with the same technical settings.

Despite such standardization of experimental conditions, some differences between the two IR algorithms were found. The first difference concerns the values of low-contrast resolution as well the sub-slice objects of 3-mm height as the supra-slice objects (see Tables 1A–3B).

Based on Figures 1–3, the effectiveness of SAFIRE (for a given iteration level) increases with a reduction of $CTDI_{vol}$, whereas the effectiveness of $iDose^4$ is nearly constant (for a given iteration level). This is evident on Figure 3 – the Pearson's coefficient for linear approximation of the relationship between reduction of $CTDI_{vol}$ and relative difference in low contrast is $R^2=0$ for iCT and $R^2=1$ for Definition AS+.

Moreover, the maximal value of $SNR(IR)/SNR(FBP)$ ratio for $iDose^4$ at level 6 is ≈ 1.8 , whereas for SAFIRE is lower at level 4 (≈ 1.6). This is true for all values of $CTDI_{vol}$.

For the highest $CTDI_{vol}$ used here (i.e. 36 mGy for iCT and ≈ 39 mGy for Definition AS+), the $SNR(IR)/SNR(FBP)$ at the highest IR level analysed in this study was ≈ 1.8 for $iDose^4$ (level 6) and ≈ 1.3 for SAFIRE (level 4).

Similar results were obtained on the basis of visualization of the smallest supra-slice low-contrast objects; a comparison between the minimal diameter of the low-contrast object visible at the FBP algorithm and that visible at the highest level of the IR algorithm is presented in Table 4.

The $iDose^4$ caused a 30% difference in the diameter, and this was constant for all $CTDI_{vol}$ levels. At the same 80% $CTDI_{vol}$ reduction, a maximal difference of 50% was found for SAFIRE (level 3).

A decreased image noise with constant radiation doses was also found by Kuo et al. [10] for the SAFIRE algorithm in comparison to FBP (both by Siemens) and also on the basis of an analysis of Catphan images.

The results indicating a possible dose reduction are also presented in the study by Ward [14], where Brilliance iCT

with an iterative algorithm was also used by the authors. In that study, clinical images of the upper abdomen of adult patients obtained with relatively low exposure parameters (120 kV, 73 mAs) were analysed and then compared to another series of images obtained with lower anode current (120 kV, 33 mAs). The latter were still considered as diagnostically acceptable. It should be underlined that the lowered anode current was preceded by analysis of Catphan 600 images, although a criterion of acceptance was the level of spatial resolution.

Conclusions

1. Both iterative algorithms definitely improve visibility of low-contrast objects in comparison to a standard algorithm (FBP) with the same exposure parameters.
2. Both iterative algorithms allow obtaining an 80% reduction of $CTDI_{vol}$ values while maintaining an acceptable visibility of low-contrast objects. At a 40% reduction of the $CTDI_{vol}$ value, the quality of images remains acceptable (visibility of low-contrast objects and SNR value).
3. The reconstruction algorithm does not have an influence on the spatial resolution value.
4. Despite the same mathematical rule of action for both compared iterative algorithms (i.e. iteration successively in the raw data domain and then in the image data domain), the results produced by the algorithms are different; $iDose^4$ effects are constant independently of $CTDI_{vol}$, whereas SAFIRE's effects become better with increasing $CTDI_{vol}$. The differences in computer programmes are probably the reason for these findings.

References:

1. Leswick DA, Hunt MM, Webster ST, Fladeland DA: Thyroid shields versus z-axis automatic tube current modulation for dose reduction at neck CT. *Radiology*, 2008; 249(2): 572–80
2. Vollmar SV, Kalender WA: Reduction of dose to the female breast in thoracic CT: A comparison of standard-protocol, bismuth-shielded, partial and tube-current-modulated CT examinations. *Eur Radiol*, 2008; 18: 1674–82
3. Willemink MJ, de Jong PA, Leiner T et al: Iterative reconstruction techniques for computed tomography. Part 1: Technical principles. *Eur Radiol*, 2013; 23: 1623–31
4. Beister M, Kolditz D, Kalender WA: Iterative reconstruction methods in X-ray CT. *Physica Medica*, 2012; 28: 94–108
5. Geyer LL, Schoepf UJ, Meinel FG et al: State of the art: Iterative CT reconstruction techniques. *Radiology*, 2015; 276(2): 339–57
6. Bittencourt MS, Schmidt B, Seltmann M et al: Iterative reconstruction in image space (IRIS) in cardiac computed tomography: Initial experience. *Int J Cardiovasc Imaging*, 2010; 27: 1081–87
7. Gervaise A, Osemont B, Lecocq S et al: CT image quality improvement using adaptive iterative dose reduction with wide-volume quality acquisition on 320-detector CT. *Eur Radiol*, 2012; 22(2): 295–301
8. Kalender WA, Beister M, Boone JM et al: High-resolution spiral CT of the breast at very low dose: concept and feasibility consideration. *Eur Radiol*, 2012; 22(1): 1–8
9. Winklehner A, Karlo C, Puippe G et al: Raw data-based iterative reconstruction in body CTA: Evaluation of radiation dose saving potential. *Eur Radiol*, 2011; 21: 2521–26
10. Kuo Y, Lin YY, Lee RC et al: Comparison of image quality from filtered back projection, statistical iterative reconstruction, and model-based iterative reconstruction algorithms in abdominal computed tomography. *Medicine (Baltimore)*, 2016; 95(31): e4456
11. Leipsic J, Labounty TM, Heilbron B et al: Adaptive statistical iterative reconstruction: Assessment of image noise and image quality in coronary CT angiography. *Am J Roentgenol*, 2010; 195: 649–54
12. Leipsic J, Labounty TM, Heilbron B et al: Estimated radiation dose reduction using adaptive statistical iterative reconstruction in coronary CT angiography: The ERASIR study. *Am J Roentgenol*, 2010; 195: 655–60
13. Pontana F, Pagniez J, Flohr T et al: Chest computed tomography using iterative reconstruction vs. filtered back projection (part 1): Evaluation of image noise reduction in 32 patients. *Eur Radiol*, 2011; 21: 627–35
14. Ward P: Munich CT study confirms value of iterative reconstruction. AuntMinnieEurope.com, 12/22/2011